THE JOURNAL OF BIOLOGICAL CHEMISTRY VOL. 285, NO. 44, pp. 34115–34125, October 29, 2010

Nuclear Factor I-C Regulates TGF-β-dependent Hair Follicle Cycling*[S]

Received for publication, March 5, 2010, and in revised form, August 4, 2010 Published, JBC Papers in Press, August 21, 2010, DOI 10.1074/jbc.M110.120659

Genta Plasari, Simone Edelmann, Florence Högger, Yves Dusserre, Nicolas Mermod[1], and Alessandra Calabrese
From the Institute of Biotechnology, University of Lausanne, 1015 Lausanne, Switzerland

Skin appendages such as teeth and hair share several common signaling pathways. The nuclear factor I C (NFI-C) transcription factor has been implicated in tooth development, but a potential role in hair growth had not been assessed. In this study we found that NFI-C regulates the onset of the hair growth cycle. NFI-C$^{-/-}$ mice were delayed in the transition from the telogen to anagen phase of the hair follicle cycle after either experimental depilation or spontaneous hair loss. Lack of NFI-C resulted in delayed induction of the sonic hedgehog, Wnt5a, and Lef1 gene expression, which are key regulators of the hair follicle growth initiation. NFI-C$^{-/-}$ mice also showed elevated levels of transforming growth factor β1 (TGF-β1), an inhibitor of keratinocyte proliferation, and of the cell cycle inhibitor p21 at telogen. Reduced expression of Ki67, a marker of cell proliferation, was noted at the onset of anagen, indicating impaired activation of the hair progenitor cells. These findings implicate NFI-C in the repression of TGF-β1 signaling during telogen stage, resulting in the delay of progenitor cell proliferation and hair follicle regeneration in NFI-C-deficient mice. Taken together with prior observations, these findings also designate NFI-C as a regulator of adult progenitor cell proliferation and of postnatal tissue growth or regeneration.

The mammalian nuclear factor I family of transcription replication factors is encoded by four genes: NFI-A, NFI-B, NFI-C, and NFI-X[2] (1, 2). NFI binding sites have been characterized in many gene promoters, where they activate or inhibit gene transcription, and NFI family members are expressed in various combinations in almost every organ and tissue (3). Distinct phenotypes and developmental defects were identified in mice knock-outs for each of the NFI genes. NFI-A-deficient mice develop neurological defects and die shortly after birth (4), whereas the absence of NFI-B provokes severe lung hypoplasia and neurological abnormalities (5). Brain malformation and severe skeletal defects were associated with NFI-X gene deficiency (6). Homozygous NFI-C knock-out mice are viable, but they have a smaller size, and tooth morphogenesis is affected. They display thin and brittle incisors and molars exhibit normal crowns but lack roots (7). These abnormalities have been associated with a decreased proliferation of NFI-C-lacking dental cells due to the overexpression of transforming growth factor β1 (TGF-β1) (8). In addition, we have also shown that NFI-C deficiency affects the normal progression of the skin wound healing process, which has been linked to altered platelet-derived growth factor (PDGF) and TGF-β signaling in the knock-out animals (9).

Tooth development shares several common stages and features with hair. Similar sets of intersecting signaling pathways, such as those elicited by TGF-β, PDGF, bone morphogenetic protein (BMP), keratinocyte growth factor, Wnt, or sonic hedgehog (Shh) have been involved in morphogenesis and maturation of these appendages in mice. Furthermore, strong evidence of the similitude of these appendages is also provided by the numerous inherited or sporadic human diseases where abnormal tooth and hair development may be attributed to the misregulation of these signaling pathways (10, 11).

Development of the murine follicles begins *in utero*. The epithelium and the underlying mesenchyme interact to form new follicles (12). After morphogenesis, each hair follicle repeatedly cycles between three stages: growth (anagen), regression (catagen), and rest (telogen) (13–15). The hair follicle is composed of three main structures. The outer root sheath (ORS) is the outer cell layer that surrounds the inner root sheath (IRS) and the hair shaft. These last two structures derive from proliferating keratinocyte progenitor cells within the hair matrix. The mesenchymal component of the follicle is the dermal papilla (DP). Composed of specialized fibroblasts, this structure connects the follicle to the bloodstream and to the nervous system. In mice, melanization is a hair follicle cycle-dependent process. Pigments are produced during the anagen phase by melanocytes dispersed among the matrix cells (16, 17).

The most distinguishable feature of the hair follicle is its continuous cyclic regeneration and formation of a new hair shaft. Stem cells leading to follicle re-growth are thought to be localized in a specialized niche within the ORS at the insertion site of the arrector pili muscle called the bulge (18). Molecular interactions between the dermal papilla and the epithelial stem cells of the bulge are believed to be responsible for activation of their proliferation, leading to the transition from telogen to anagen phase. The stimulation of bulge stem cells gives rise to rapidly dividing cells that migrate to the matrix (18). These keratinocyte progenitor cells will undergo a finite number of divisions to generate the lower part of the follicle, where their terminal differentiation will produce the IRS and the hair shaft (19).

The molecular nature of the epithelial-mesenchymal crosstalk leading to the transition from a quiescent to a proliferative

* This work was supported by the University of Lausanne.
[S] The on-line version of this article (available at http://www.jbc.org) contains supplemental Table 1 and Figs. 1–3.
[1] To whom correspondence should be addressed: Laboratory of Molecular Biotechnology, Station 6, 1015 Lausanne, Switzerland. Tel.: 41-21-693-61-51; Fax: 41-21-693-76-10; E-mail: Nicolas.Mermod@unil.ch.
[2] The abbreviations used are: NFI, nuclear factor I; BMP, bone morphogenetic protein; Shh, sonic hedgehog; ORS, outer root sheath; IRS, inner root sheath; DP, dermal papilla; Bicine, *N*,*N*-bis(2-hydroxyethyl)glycine; GGT, γ-glutamyl transpeptidase; K15, keratin 15; qPCR, quantitative PCR.

phase is poorly understood. However, several genetic studies have suggested that the hair follicle transition from telogen to anagen is associated with a series of events involving the inhibition of BMP pathways (20) and the activation of Shh, Wnt/β-catenin/Lef-1 and STAT3 signaling (21–24). BMP4 was identified as an inhibitor of the hair follicle cycle progression that is responsible for the maintenance of the follicle in the telogen phase (20, 25). The anagen onset was associated to an inhibitor-releasing mechanism involving *de novo* expression of Noggin, which acts by antagonizing BMP4 signaling. Inactivation of the BMP4 signal coincides with the induction of the Shh signaling, which in turn activates the Wnt/β-catenin/Lef-1 pathway, cell proliferation, and hair shaft formation (26–29). At the end of anagen, the transition of actively growing hair follicles into the phase of spontaneous involution (catagen) is characterized by the increase of TGF-β1 signaling, which drives apoptosis and proliferation arrest of the keratinocytes in the hair follicle matrix and epithelial strands (12, 30).

While studying the role of NFI-C on skin wound healing (9), we observed a previously unidentified phenotype related to a hair growth delay in NFI-$C^{-/-}$ mice. Examination of the hair follicle cycle in NFI-C wild-type and knock-out mice indicated that the telogen-anagen transition is delayed in NFI-$C^{-/-}$ mice. Consistently, decreased expression of Shh and Wnt5a at anagen onset and of Lef1 during the growing phase was found in knock-out mice, implying NFI-C in the regulatory events that lead to anagen onset. High levels of TGF-β1 and cell cycle inhibitor p21/WAF1/CIP1 (p21) and decreased expression of Ki67, a marker of cell proliferation, were observed at the telogen and telogen-anagen transition in NFI-$C^{-/-}$ animals. Taken together, these results indicate that loss of NFI-C leads to a persistent activation of the TGF-β pathway at telogen that induces a delay in Shh and Wnt/β-catenin/Lef-1 signaling activation and keratinocyte proliferation.

EXPERIMENTAL PROCEDURES

Animal Care and Experimentation—NFI-C knock-out mice generated by removal of the second exon from NFI-C gene were kindly provided by Gronostajski and co-workers (7), and NFI-C-null animals were obtained by breeding heterozygous littermates. All mice in this study have the C57Bl/6 background and were housed in a temperature-controlled room (23 °C) on a 12-h dark/12-h light cycle. As homozygous knock-out animals have brittle teeth, a ground standard rodent chow (Kliba Nafag) as well as the unground chow and water was provided *ad libitum* to all animals under study three times a week after weaning (P21).

Hair Follicle Cycle Induction—Over-groomed litters were separated from the mother 28 days after birth. The day of weaning was considered as day 0 after over-grooming, after which skin biopsies were collected to study fur recovery in wild-type and knock-out animals. Alternatively, non-over-groomed 23-day-old mice were depilated using a wax/rosin mixture to induce and synchronize hair follicle cycling in the plucked area (14). Skin biopsies were collected from the depilated area to perform histological sections, or they were snap-frozen in liquid nitrogen for gene expression analysis. Each time point after plucking was analyzed in triplicate on NFI-$C^{-/-}$ or wild-type mice. Differences between the timing of spontaneous anagen stages of NFI-$C^{-/-}$ and wild-type animals was detected similarly up to 28 days after birth.

Immunohistochemistry—Hematoxylin/eosin staining was performed on 5-μm paraffin sections of back skin. The endogenous alkaline phosphatase activity was detected using the Vector Black Alkaline Phosphatase Kit II (Vector Laboratories). Briefly, the enzyme substrate was applied directly on 7-μm skin cryosections and incubated for 20 min at room temperature to develop a brown/black reaction product. P-cadherin immunostaining was performed on 7-μm cryosections of back skin fixed for 3 min in 100% ethanol using a rat monoclonal antibody (PCD-1, Takara) at a 1/1000 dilution for 2 h and an anti-rat IgG secondary FITC-conjugated antibody (Santa Cruz Biotechnology). For K15 immunofluorescence, cryosections were fixed for 3 min in 100% acetone and incubated overnight with the blocking solution from the MOM kit of Vector Laboratories diluted at 1/10. Slides were successively incubated for 2 h with a mouse monoclonal anti-K15 (LHK15, Novocastra) at a 1/100 dilution and an anti-mouse secondary antibody Alexa 546-conjugated (Molecular Probes). The immunostaining for Ki67 and p-Smad2/3 was performed on 4% paraformaldehyde fixed paraffin sections of back skin. Slides stained for Ki67 were subjected to epitope retrieval by immersion in 10 mM citrate buffer, pH 6.0, and heated for 20 min in a microwave oven set to 800 watts. Incubation with the anti-Ki67 goat antibody (Santa Cruz Biotechnology) was performed overnight, and detection was carried-out with anti-goat antibody coupled to biotin (Santa Cruz Biotechnology). Revelation was performed with a FITC-conjugated streptavidin (Vector Laboratories). P-Smad2/3 stained slides were incubated with p-Smad2/3 goat antibody (Santa Cruz Biotechnology) for 1 h, and detection was performed with anti-goat antibody coupled to biotin (Santa Cruz Biotechnology) and the VECTASTAIN® ABC kit (Vector Laboratories). Revelation was performed with diaminobenzidine (Sigma). All sections were counterstained with DAPI to visualize cell nuclei and photographed using light, fluorescence, or confocal microscopy. The number of p-Smad2/3-positive cells residing in the hair follicle was evaluated from three knock-out and wild-type mice. A total of about 50 hair follicles per day were analyzed for each group of mice. A statistical analysis was performed using a two-tailed, two-sample equal variance *t* test.

γ-Glutamyl Transpeptidase (GGT) Enzymatic Assay—GGT enzyme activity was measured as described previously (31, 32). Briefly, 200-μm skin sections were homogenized in 50 μl of buffer containing 10% glycerol, 1% Triton, and 5 mM K_2HPO_4 at pH 7. The suspensions were centrifuged, and the total protein concentration of the supernatants was measured using a Bradford assay. A volume of 10 μl of the supernatant was used for the enzymatic assay with 100 μl of substrate buffer containing 1.26 mg/ml γ-glutamyl-nitro, 2.92 mg/ml glycylglycine, 11 mM HCl_2, and 50 mM Bicine. Reactions were incubated at 25 °C for 2.5 h, after which they were stopped by adding 100 μl of 4.4 M acetic acid. The yellow reaction product was quantified by spectrophotometry at 410 nm. Sample absorbance values were normalized to the total protein content after deduction of the background absorbance obtained with 10 μl of supernatant inactivated by prior incubation at 100 °C. A standard curve of

GGT activity was established using a range from 0 to 2×10^{-4} units of equine kidney GGT (Sigma), and the GGT skin activity is expressed as units per μg of extract total proteins. Statistical significance of enzyme activity differences was determined using a two-tailed paired *t* test.

RNA Extraction and Real Time PCR Analysis—Total RNAs were extracted from whole thickness skin explants using TRIzol (Invitrogen) according to the manufacture's instructions. Further purification of RNA was performed using RNeasy Mini kits (Qiagen). RNA integrity was assessed by electrophoresis on a 1% agarose gel and ethidium bromide staining. Reverse transcription was performed using RT-PCR Master Mix (GE Healthcare). Briefly, 1 μg of total RNA was reverse-transcribed with random primers, and first strand reverse-transcribed cDNA was diluted 1:200 in water before use. Real-time PCR was carried out with LightCycler 480 SYBR Green I Master kit using a LightCycler 480 system (Roche Applied Science) as recommended by the manufacturer. Relative gene expression was calculated using the equation E_B^{CtB}/E_A^{CtA}, where E represents the efficiency as estimated with the LinReg method, Ct is the threshold cycle, *B* is the endogenous reference, and *A* is the gene of interest as described previously (33). As the endogenous reference, we used the geometric mean of the mRNA levels of the eukaryotic elongation factor 1 α1 (EEF1a1) and ribosomal protein S9 (RPS9). Primer sequences are listed in supplemental Table 1. The results represent the mean of three animals ± S.E. Statistical significance of differences in gene expression was examined using a two-tailed, two-sample equal variance *t* test.

RESULTS

Identification of a Delayed Hair Growth Phenotype in NFI-C$^{-/-}$ Mice—Hair barbering of a litter is a stress-related disorder observed with some inbred mouse lines that appears as a loss of hair of all pups as a consequence of an over-grooming behavior by the mother. This was occasionally observed during the breeding of NFI-C knock-out heterozygote mice, which resulted in a similar loss of the fur for all littermates irrespective of their genotype. All mice recovered their fur after weaning and separation from the mother. However, fur recovery was delayed for the NFI-C$^{-/-}$ mice when compared with wild-type or heterozygous littermates (Fig. 1*A*). A histological study of the skin structure at the time of weaning (day 28 post-partum) revealed invaginations of the epithelium in the dermis and broken hair shafts (Fig. 1*B*). These invaginations were observed in the skin of both wild-type and knock-out mice, suggesting that they may result from over-grooming. The repetitive licking by the mother may have caused a weakening of the hair shaft and its rupture within the follicle sheath. Animals of both genotypes eventually recovered normal skin and follicular structures, although at a different pace, as demonstrated by histological studies of the skin 15 days post-weaning (Fig. 1*C*). The hair follicles had developed and the epidermis was reconstituted, as invaginations were no longer visible in both types of skins. At this time, wild-type mouse follicles had already reached the telogen phase, characterized by thinner and shorter follicles, whereas the follicles of NFI-C-deficient mice were still in anagen phase, as follicles were well developed and the bulbs resided in the deep subcutis. Thus, NFI-C$^{-/-}$ mice showed a delay in

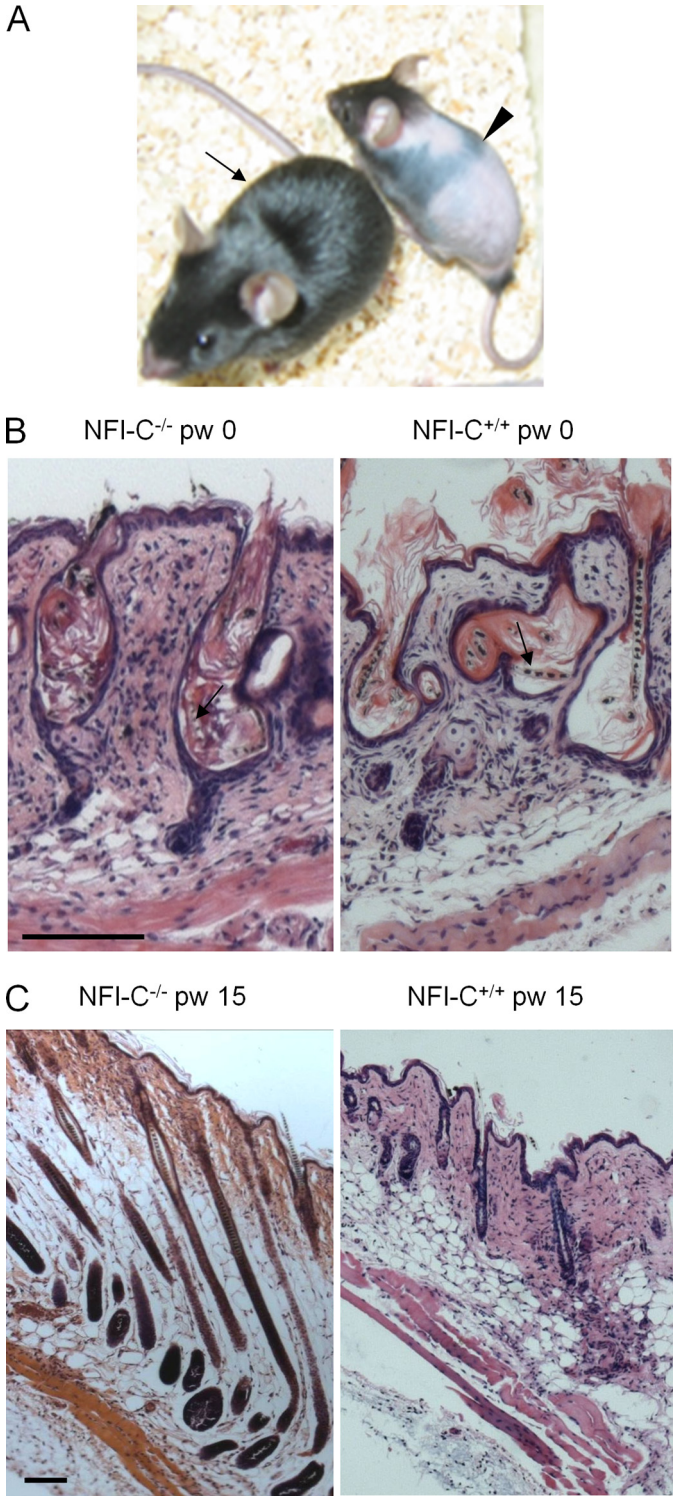

FIGURE 1. **Hair growth delay phenotype identified in over-groomed NFI-C$^{-/-}$ mice.** *A*, observation of the hair growth 10 days after weaning in an over-groomed litter is shown. The wild-type mouse recovered its normal fur (*arrow*), whereas the knock-out animal still exhibited a hairless body (*arrowhead*). *B*, hematoxylin eosin staining of skin sections performed at weaning (*pw 0*) and 15 days post-weaning (*pw 15*) are shown. *Arrows* indicate the broken hair shafts within the follicle epithelium of telogen phase hair follicles from sections of wild-type and knock-out mice at weaning, probably as a result of the repetitive licking of the fur and skin. *C*, representative illustrations of normal hair follicle structures 15 days after weaning are shown. Note the telogen phase wild-type hair follicles, as characterized by thin follicles, whereas those of NFI-C-null mice were still in anagen. *Scale bars*: 100 μm.

the follicle growth and formation of the new hair shaft, suggesting a role for NFI-C in hair follicle regeneration.

NFI-C Regulates the Hair Follicle Cycle but Not Morphogenesis—To avoid potential side effects of over-grooming and to ascertain the involvement of NFI-C in the growth of normally structured follicles, we used the depilation-induced hair follicle cycling model. This consists of hair removal by the plucking of all hair shafts from the back of 23-day-old mice, which has been shown to induce homogenous and synchronized transition from the first telogen phase to anagen over the entire depilated skin area (14). Eight days after plucking, the depilated skin areas of control mice were gray, indicating melanization, whereas those of mutant mice were pink (Fig. 2*A*). No difference was noted when comparing wild-type and heterozygous mice (data not shown). In mouse skin, melanin production depends on the progression to anagen phase, as it is mainly synthesized by the melanocytes within the growing hair bulb (16). The hair cycle was delayed but not abolished in knock-out animals, as they showed a similar gray coloration 2–3 days later (data not shown). Knock-out animals eventually recovered their entire fur in the depilated area with no difference in structure, size, and number of the new hair follicles as compared with wild-type mice (data not shown). This confirmed a hair growth delay of NFI-C$^{-/-}$ mice independently of over-grooming.

To identify the delayed hair follicle cycle stage, we next performed hematoxylin-eosin staining of skin biopsy sections collected during the first 8 days after plucking. The first differences in follicle growth could be observed at day 4 post-depilation when comparing NFI-C-expressing and homozygous knock-out mice (Fig. 2*B*). Although wild-type follicles reached anagen III, the stage at which new bulbs reach the border between the dermis and hypodermis (14), knock-out follicles were still in telogen or just entering anagen (Fig. 2*B*). This result suggested that it is the hair cycle initiation step that is delayed in NFI-C-null mice. As this might result from the increased inflammation reaction induced by plucking (34), we examined the spontaneous hair growth at anagen 28 days post-partum. Although the hair follicle cycle generally depends on the genetic background, sex, environment, and nutritional factors, morphogenesis as well as the first postnatal cycle (catagen, telogen, and anagen) follow a rather precise and synchronized time-scale. As for the plucking-induced anagen experiments, a delayed spontaneous growth was observed in knock-out animals, implying again an inefficient onset of the anagen phase (Fig. 2*C*). At day 28 post-partum, the wild-type mouse follicles followed a normal cycle course and transition to the anagen phase, whereas knock-out mouse follicles were still in telogen and exhibited a thinner skin.

These findings indicated that there is a general delay of the telogen to anagen phase transition in knock-out mice that occurs independently of the hair removal procedure. To assess whether cycle retardation may result from a general defect in hair morphogenesis, we performed hematoxylin-eosin staining of skin sections collected at day 2.5, 4, 6, and 9 post-partum from NFI-C-deficient and wild-type mice. Interestingly, no difference in follicular morphogenesis was observed between the two genotypes (data not shown), indicating that follicle development *per se* is not affected by the lack of NFI-C. Overall, these

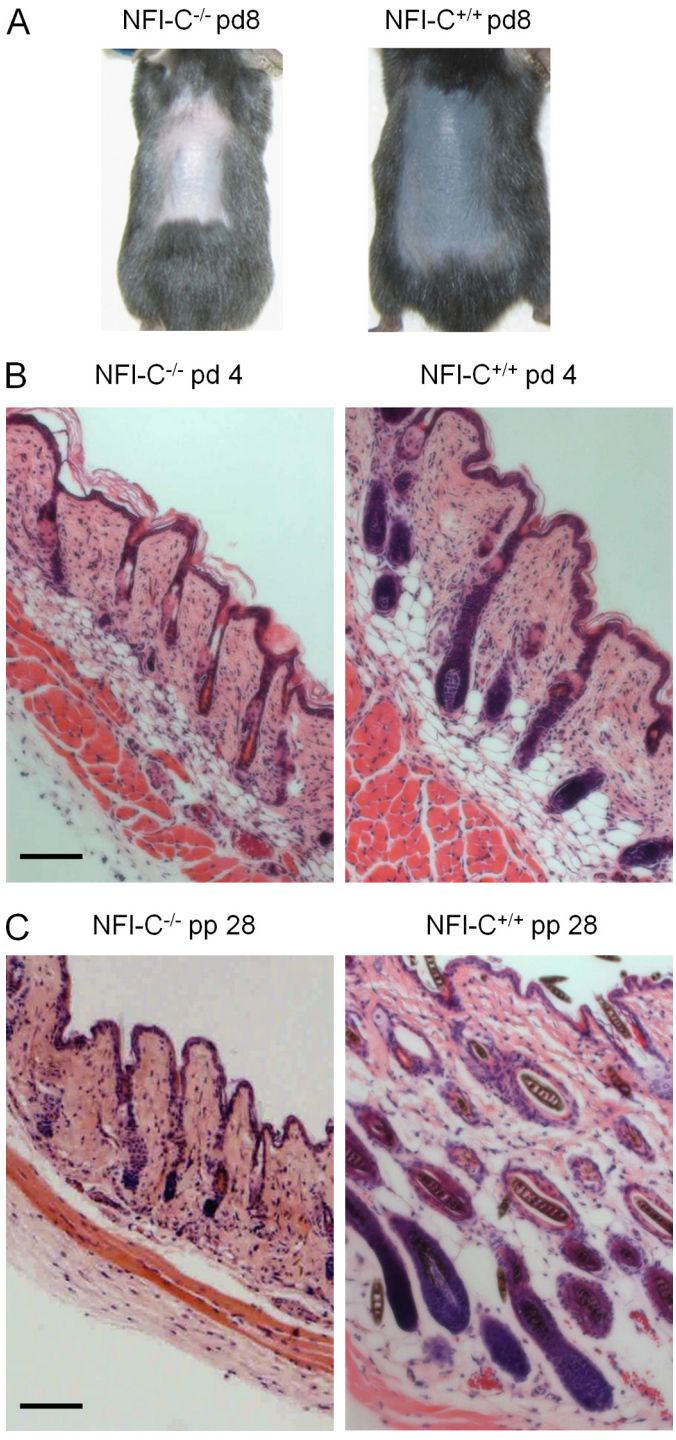

FIGURE 2. **NFI-C is involved in the hair follicle cycling.** *A*, 8 days after hair depilation, hair growth was delayed in NFI-C$^{-/-}$ mice, as evidenced by the difference of the back skin color. Note the gray-colored skin of wild-type mice typical of anagen phase pigmentation, whereas the knock-out mice still displayed a pink-colored skin. *B*, 4 days after depilation (*pd 4*), the hematoxylin eosin staining of skin histological sections reveals wild-type follicles in early anagen, as indicated by their location at the border between the dermis and the subcutis and the increased size of dermal papillae. In contrast, mutant follicles are just entering anagen and are still located in the dermis. *C*, shown is hematoxylin eosin staining of histological sections performed at day 28 post-partum (*pp 28*) of skins not submitted to over-grooming or depilation. Progression to anagen during spontaneous activation of the follicle cycle is delayed in knock-out *versus* normal animals, as evidenced by the different structure and location of hair follicles. Whereas wild-type animals progressed to the anagen phase, mutant mice are still in telogen. *Scale bars*: 100 μm.

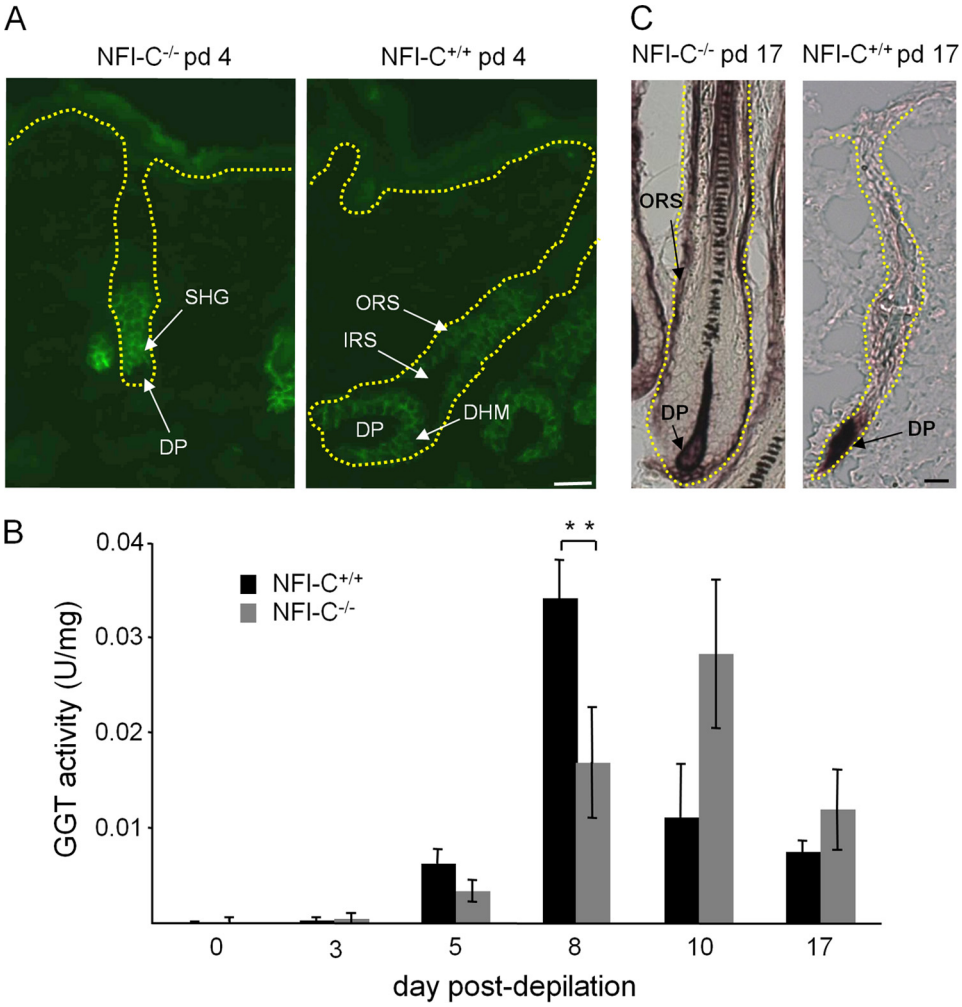

FIGURE 3. **NFI-C-null mice have delayed anagen onset but otherwise normal hair follicle cycle progression.** Molecular markers of the hair follicle cycle progression were analyzed in histological sections of skin collected along the cycle at the indicated days post-depilation (*pd*). *A*, 4 days after depilation, the wild-type follicles exhibited a staining typical of the anagen III stage, with P-cadherin being expressed in ORS and matrix but not in the IRS. The knock-out follicle showed a staining typical of the telogen phase as only the secondary hair germ exhibits a strong staining. *B*, γ-glutamyl transpeptidase colorimetric assay was carried on extracts of skins collected at various times after depilation to encompass the first hair follicle cycle of normal and mutated animals. The *error bars* represent S.E.; **, indicates $p < 0.01$. *C*, staining for the alkaline phosphatase activity was similar in the dermal papilla (*DP*) of knock-out and wild-type 17 days after plucking. Knock-out animals displayed an additional staining in the ORS characteristic of the end of catagen, whereas wild-type follicles entering telogen do not. The *yellow dashed lines* indicate the limit of keratinocyte epidermal layers determined by contrast phase. *DHM*, developing hair matrix; *SHG*, secondary hair germ. *Scale bars*: 20 μm.

findings indicate that the retarded hair growth observed in knock-out animals resulted from a delayed step during or preceding the initiation of anagen.

NFI-C Regulates the Hair Follicle Telogen to Anagen Transition—The successive increase and decrease of follicular length during the hair cycle is accompanied by drastic changes in protein levels, which can be used to distinguish specific stages of the cycle. To further examine the hair growth delay in NFI-$C^{-/-}$ animals, we performed immunostaining of P-cadherin, a cell-cell adhesion molecule expressed in a subset of follicular cells. P-cadherin was present in the ORS and in keratinocytes of the developing hair matrix (*DHM*) but not in the IRS and DP of wild-type animals at day 4 post-depilation (Fig. 3*A*), as expected from Müller-Röver *et al.* (35). In contrast, P-cadherin was only detected in the secondary hair germ in knock-out littermates. Thus, knock-out mouse hair follicles are delayed at an early step of anagen, whereas the wild-type follicle cycle follows a normal timing.

GGT is a metabolic enzyme that contributes to the transfer of γ-glutamyl groups on peptides and L-amino acids (36, 37). In healthy skin GGT activity is present exclusively in the ORS and IRS of the hair follicle during anagen, whereas it is absent from the epidermis, dermis, and hypodermis. GGT activity increases during anagen and gradually regresses in catagen to reach undetectable levels in telogen, providing a reliable indicator of the cycle progression after plucking (38). Wild-type depilated mice exhibited normal hair follicle cycle timing as detected from the GGT activity, whereas that of NFI-$C^{-/-}$ mice followed a similar profile but reached a maximum ~2 days after their wild-type counterparts (Fig. 3*B*).

The expression and localization of alkaline phosphatase are also hair cycle-dependent, as the DP displays elevated activity during the entire hair cycle, whereas the ORS expresses this protein during late anagen and catagen (39). Thus, the alkaline phosphatase activity was measured to investigate if the follicular cycling delay also occurred at the end of the cycle. As expected, a high activity was observed in the DP of both genotypes. However, alkaline phosphatase activity was only observed in the ORS of knock-out follicles (Fig. 3*C*). Although NFI-C-deficient follicles were in catagen, normal follicles were finishing the cycle and entering telogen, as the apoptotic strand of keratinocytes had lost staining for alkaline phosphatase and dermal papillae were reduced in size. Overall, we conclude that the delay occurring at the onset of anagen in knock-out mice persists until the completion of the hair cycle. Thus, NFI-C is specifically involved in the control of the timing of hair cycle initiation but not in follicular growth or morphogenesis.

Molecular Events Mediating Follicular Growth Delay of NFI-$C^{-/-}$ Mice—We next assessed whether NFI-C may modulate the signaling pathways that control the hair follicle cycling. The transcript levels of various signaling intermediates linked to anagen onset were quantified by real-time PCR analysis of skin biopsies, and levels were normalized to those of a collection of reference genes whose expression was found to be robust and

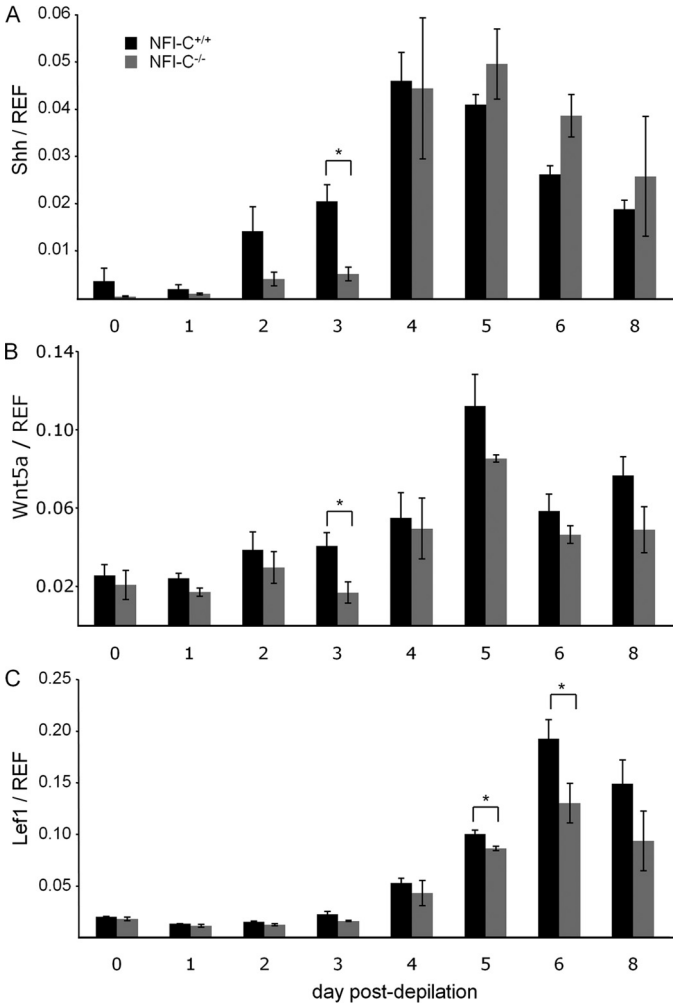

FIGURE 4. **NFI-C$^{-/-}$ mice display altered signaling pathways controlling anagen onset.** The expression levels of Shh (*panel A*), Wnt5a (*panel B*), and Lef1 (*panel C*) relative to reference (*REF*) genes were assayed by RT-qPCR performed on extract from skin biopsies collected to the indicated time points after depilation. *, indicates $p < 0.05$.

invariant during the hair follicle cycle.[3] High Shh expression was observed in wild-type animals at the onset of anagen 4 days after depilation followed by a gradual decrease (Fig. 4*A*), as expected from previous studies linking the hair follicle transition from telogen to anagen to the activation of the Shh pathway (24, 40, 41). In knock-out animals, the expression of Shh remained significantly lower until day 3 post-depilation but eventually reached wild-type levels at day 4.

Wnt5a expression was shown to be controlled by Shh signaling (22). Consistently, we identified an increase of Wnt5a expression up to day 5 post-depilation, 1 day later than the peak of Shh gene expression (Fig. 4*B*). NFI-C-null animals displayed significantly lower expression of Wnt5a at day 3 post-depilation, which corresponds well with the lower expression of Shh gene in knock-out mice. The Shh- and Wnt-activated cascade leads to β-catenin release, stabilization, and nuclear translocation, where it interacts with the Lef1 transcription factor to induce expression of hair keratin genes in proliferative matrix cells and precursors of the hair shaft (42, 43). Consistently, maximal Shh expression at day 4 correlated well with the Lef1 expression increase in wild-type mice, whereas a slower increase of Lef1 expression occurred during anagen at days 5 and 6 in knock-out mice (Fig. 4*C*). This tallies with the lower expression of Wnt5a in knock-out animals, as Wnt-responsive elements have been identified in the Lef1 promoter (43, 44). The expression pattern of Shh, Wnt5a, and Lef1 in knock-out mice and their role in promoting anagen onset, thus, provides a rationale for the retarded regeneration of the lower part of the follicle. Taken together, these results indicate that loss of NFI-C impairs the timing of Shh expression onset rather than its expression level and that this may result in abnormally low Wnt5a and Lef1 levels.

NFI-C Represses TGF-β1 Pathway during Telogen Phase—Activation of Shh pathway results from the relief of BMP4 inhibitory effects at late telogen, during which signals elicited by its binding to BMPR-IA prevent the onset of anagen. At anagen onset, increased levels of Noggin, a BMP antagonist, relieve this inhibition and trigger the activation of the growth phase (24, 40, 41). Expression of BMP4 was found to decrease gradually up to 3 days after plucking, and that of Noggin showed a comparable peak of expression in NFI-C knock-out and wild-type skin biopsies (supplemental Fig. 1). Similarly, no significant changes were observed in the expression of PDGFA, PDGF-Rα, keratinocyte growth factor, or TGF-βRII in wild-type and knock-out skins (data not shown). In contrast, highly significant differences were found in the expression levels of TGF-β1. At days 0, 1, and 2 post-depilation, knock-out animals showed more elevated levels of the growth factor compared with their wild-type littermates (Fig. 5*A*). We also observed a significant increase of TGF-β1 levels at day 1 compared with day 0 in both genotypes ($p < 0.01$), possibly due to the injury applied by the depilation protocol. Phosphorylation of Smad2 and -3 is a direct effect of TGF-β1 pathway activation (45). Consistently, we found an increased number of p-Smad2/3-positive keratinocytes in the ORS of knock-out follicles at day 1 after depilation (Fig. 5, *B* and *C*).

Stimulation of TGF-β1 signaling has been shown to control the catagen stage through induction of apoptosis and inhibition of keratinocyte proliferation (12, 30). Thus, TGF-β1 is expected to be down-regulated during telogen and anagen phases to allow progenitor keratinocytes to grow. The high levels of the growth factor found in knock-out animals indicates that NFI-C is implicated in the control or in the modulation of the TGF-β1 pathway and that it may act to repress the signaling after the regression phase. We, thus, tested NFI-C expression over the entire follicular cycle, and we found a markedly elevated expression at the end of telogen and at the anagen-telogen transition (day 0–2 post-depilation) when compared with the anagen phase (day 3–8) (Fig. 5*D*). This implies that NFI-C is required during the resting phase and anagen onset to repress TGF-β1 signaling. Thus, loss of NFI-C causes a prolonged expression of TGF-β1 and a consequent delay in the re-initialization of hair follicle cycle.

[3] G. Plasari, S. Edelmann, F. Högger, Y. Dusserre, N. Mermod, and A. Calabrese, unpublished results.

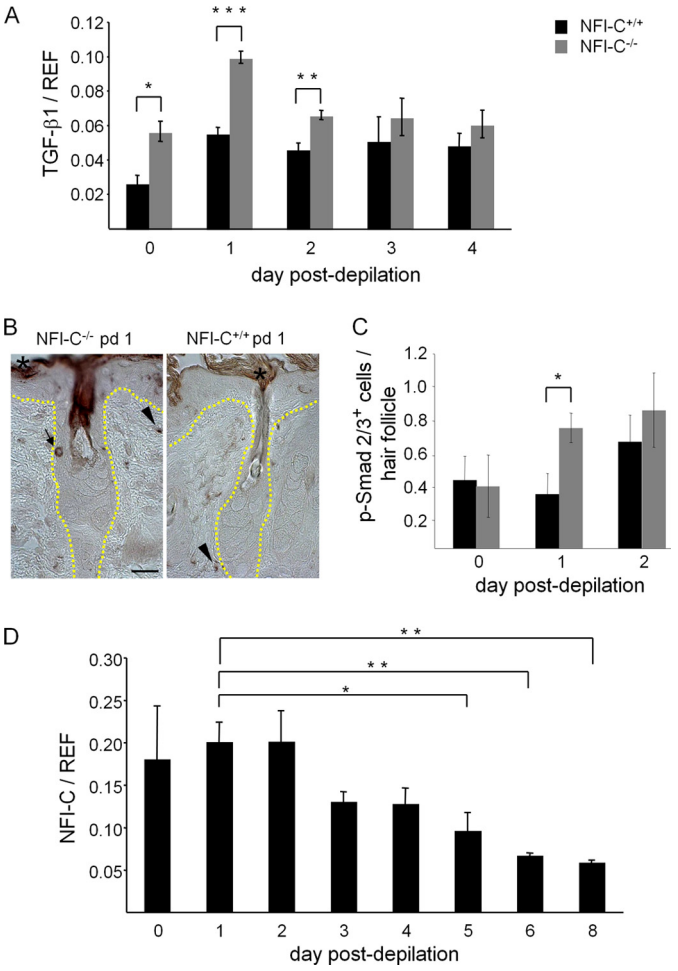

FIGURE 5. **NFI-C controls TGF-β1 levels during telogen phase.** *A*, TGF-β1 expression relative to reference (*REF*) genes assayed on total skin extract by RT-qPCR at the indicated days after the depilation. *B*, immunostaining of p-Smad2/3 at day 1 post-depilation. A positive cell in the ORS of knock-out hair follicle is indicated by an *arrow*, whereas no staining was detected in wild-type follicular keratinocytes. *Arrowheads* indicate positive dermal fibroblasts. A nonspecific brown staining was detected in the corneal layers (*asterisks*). The *yellow dashed lines* indicate the limit of the keratinocyte epidermal layer. *Scale bar*: 25 μm. *C*, the average number ± S.E. of p-Smad2/3-positive cells per hair follicle was calculated in knock-out and wild-type mice at day 0 to day 2 post-depilation. *D*, NFI-C mRNA expression was assessed by the RT-qPCR assay of extracts of skin biopsies from wild-type animals collected at the indicated time points after depilation. NFI-C expression levels were significantly more elevated during telogen or the telogen-anagen transition (days 0–2) as compared with anagen (days 5–8). *, $p < 0.05$; **, $p < 0.01$; ***, $p < 0.001$.

TGF-β1 Pathway Activation and Increased p21 Expression Accompany a Decreased Proliferation of Knock-out Progenitor Cells—Epithelial hair follicle stem cells are located at the insertion site of the arrector pili muscle in a specialized portion of the ORS called the bulge from which they proliferate and migrate to the hair matrix during anagen in a tightly regulated and coordinated process (19). TGF-β has been shown to inhibit the growth of epithelial cells by controlling the cell cycle progression. p21 is a well characterized cyclin-dependent kinase inhibitor whose up-regulation has been associated with the growth inhibitory effect of TGF-β1 (45). Thus, we next assessed whether the altered TGF-β1 signaling in NFI-C knock-out animals may have affected the expression of p21 and progenitor cell division. A significant up-regulation of p21 expression was observed after depilation and the following day, consistent with the high levels of TGF-β1 during the telogen phase (Fig. 6*A*). To evaluate the effect of the misregulated p21 expression, we measured the Ki67 cell proliferation marker in normal and knock-out follicles at the early and late anagen stages. At day 0, 1, and 2 after depilation, the hair follicle cells of both genotypes were in the quiescent telogen phase, as no Ki67-positive cells were detected (data not shown). However, proliferating cells were observed in wild-type follicles within the secondary hair germ surrounding the dermal papilla at day 3, as an early event of anagen onset (Fig. 6*B*). At day 4, the wild-type hair matrix cells were found to proliferate actively within the newly constituted lower part of the follicle (Fig. 6*C*). In contrast, no proliferating cells were observed at day 3 in NFI-C-deficient follicles, and weak staining of the secondary hair germ was detectable at day 4 (Fig. 6, *B* and *C*). Ki67 staining performed at day 8 post-depilation showed high expression in the nuclei of hair matrix cells of both genotypes (Fig. 6*D*). Thus, knock-out mice showed no global perturbation of the proliferation of the cells known to give rise to the IRS and hair shaft lineages at late anagen. We next assessed the *in vitro* proliferation activity of primary keratinocytes in response to TGF-β1 (supplemental Fig. 2). Keratinocytes of both genotypes showed a similar decrease of proliferation when TGF-β1 was added to the culture medium, demonstrating that the NFI-C-deficient cells are not intrinsically impaired in cell division *per se* nor in the signaling pathway elicited by TGF-β1 to repress cell proliferation. Because TGF-β is known to induce apoptosis (45), we evaluated the number of apoptotic hair follicle keratinocytes at days 0–3 and 10 after plucking (supplemental Fig. 3). A low amount of dead cells was detected at the beginning of the cycle compared with day 10 (catagen phase for wild-type mice), and no significant difference was seen between the two genotypes, suggesting that the increased levels of TGF-β1 in NFI-C$^{-/-}$ mice are not sufficient to trigger the apoptotic process. These results taken together indicate that impaired TGF-β pathway regulation results in an up-regulation of a cell cycle inhibitory protein, which in turn may provoke the prolonged quiescence of the NFI-C-deficient follicular stem and/or progenitor cells.

Keratin 15 (K15) is a follicular stem cell marker whose mRNA and protein are reliably detected in the bulge where it is expressed at high levels, whereas lower levels were occasionally detected in the basal layers of the follicle ORS and in the epidermis (46). In addition, K15 expression was shown to be down-regulated by TGF-β1 after a cutaneous injury (47). This prompted us to assess the levels of K15 during the first part of the hair follicle cycle. As expected, we found a strong decrease of the stem cell marker levels at day 1 post-depilation in both genotypes due to the increased expression of TGF-β1 (Fig. 7*A*). In addition, at this time point the mRNA levels of K15 in wild-type animals were significantly higher than those of knock-out mice. Three days after depilation, NFI-C$^{-/-}$ mice showed a moderate but nevertheless significant increase of K15 mRNA levels as compared with day 1 and to the wild-type littermates, indicating again a correlation between K15 expression and the decreased levels of TGF-β1 from day 1 to day 3 post-depilation in NFI-C null mice (Fig. 7*A*).

This suggested that NFI-C might not merely regulate the onset of cell proliferation but also the reservoir of stem cells

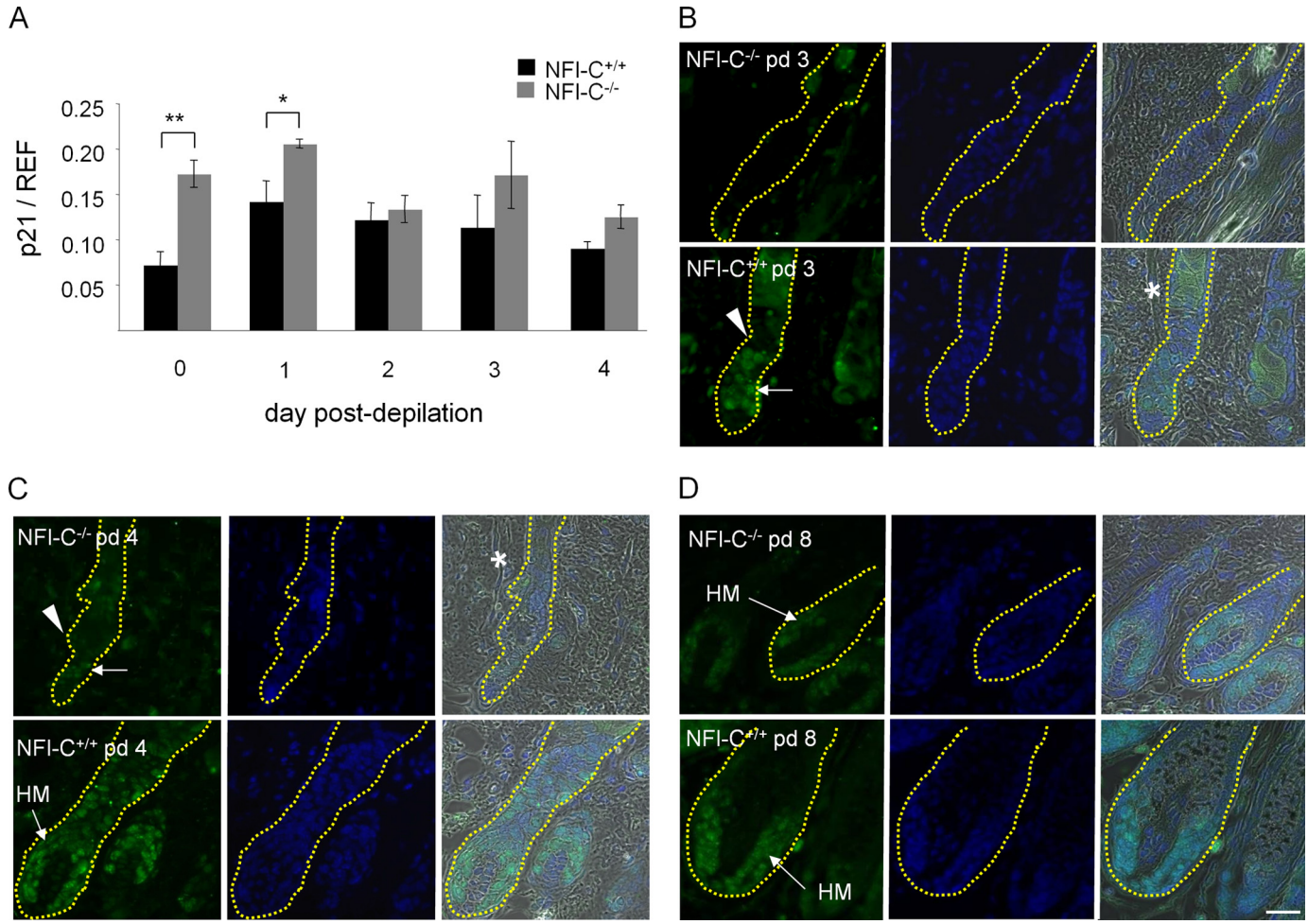

FIGURE 6. **NFI-C regulates the expression of cell cycle inhibitor p21 and the activation of keratinocyte proliferation at anagen onset.** *A*, p21 mRNA levels were analyzed by RT-qPCR in samples of skin collected from day 0 to day 4 after depilation and they were normalized to reference (*REF*) mRNAs. A significant increase of p21 was observed at days 0 and 1 in knock-out mice compared with wild-type littermates (*, $p < 0.05$; **, $p < 0.01$). *B–D*, keratinocytes were labeled for Ki67 antigen at day 3 (*B*), day 4 (*C*), and day 8 (*D*) post-depilation (*pd*). Nuclei were stained with an antibody against Ki67 (*green*) and DAPI (*blue*), and the phase contrast, Ki67, and DAPI signals are merged. The *asterisks* show the location of the arrector pili muscle, whereas the *yellow dashed lines* indicate the limit of keratinocyte layer. At days 3 and 4, proliferating cells of the secondary hair germ positive for Ki67 are indicated by *arrows*, whereas the Ki67-negative slow cycling cells of the bulge were shown by the *arrowhead*. No proliferative signal was observed at day 3, and a weak signal was detected at day 4 in mutant mice. At days 4 and 8, keratinocytes that proliferate in the hair matrix (*HM*) to form the new shaft are indicated by the HM-labeled *arrows*. *Scale bar*: 25 μm.

that gives rise to the hair follicle structure. This was addressed using K15 immunofluorescent staining of skin cryosections along progression to anagen. K15 staining was easily detectable in the bulge/secondary hair germ, ORS, and basal layer of epidermis at days 0 and 1 post-depilation (Fig. 7*B* and data not shown). Consistent with the mRNA levels, K15 staining was decreased at day 2 after depilation, and its expression was most prominent in the bulge/secondary hair germ area and barely detectable, if at all, in the basal layer of the ORS and in the epidermis. In contrast, no difference was observed in the expression level or distribution of K15 in the wild-type and knock-out follicular cells, implying similar numbers of stem cells. Taken together, these results indicate that NFI-C is mainly involved in the activation of progenitor cell division rather than in the control of stem cell amount or distribution.

DISCUSSION

Skin appendages such as teeth and hair follicles share many common features and similar signaling during organ morphogenesis. However, the specific signals that mediate the continuous growth of mouse teeth or the cycling of hair growth remain poorly understood. Here we report a delayed hair follicle cycle in NFI-C-lacking mice. This hair growth phenotype was first observed in litters subjected to over-grooming, which is a stress-related disorder that leads to a loss of body hairs elicited by excessive mother care during lactation. After weaning, all mice recover their fur, but recovery is delayed in knock-out animals when compared with wild-type littermates. Consistently, follicular cycling was also delayed in the knock-out animals compared with wild type after hair plucking, indicating that the phenotype does not result from over-grooming *per se*.

Hair plucking induces tissue damages and it activates an inflammatory reaction that promotes entry of the quiescent hair follicles in a proliferative stage (48). Proinflammatory cytokines or growth factors released after plucking may be responsible for anagen phase induction. For instance, PDGF, a potent chemotactic agent for macrophages, is known to activate the growth of telogen follicles (49). We recently found that NFI-C is involved in the inflammatory phase of the skin healing process (9). The PDGF and TGF-β1 pathways were both found to be

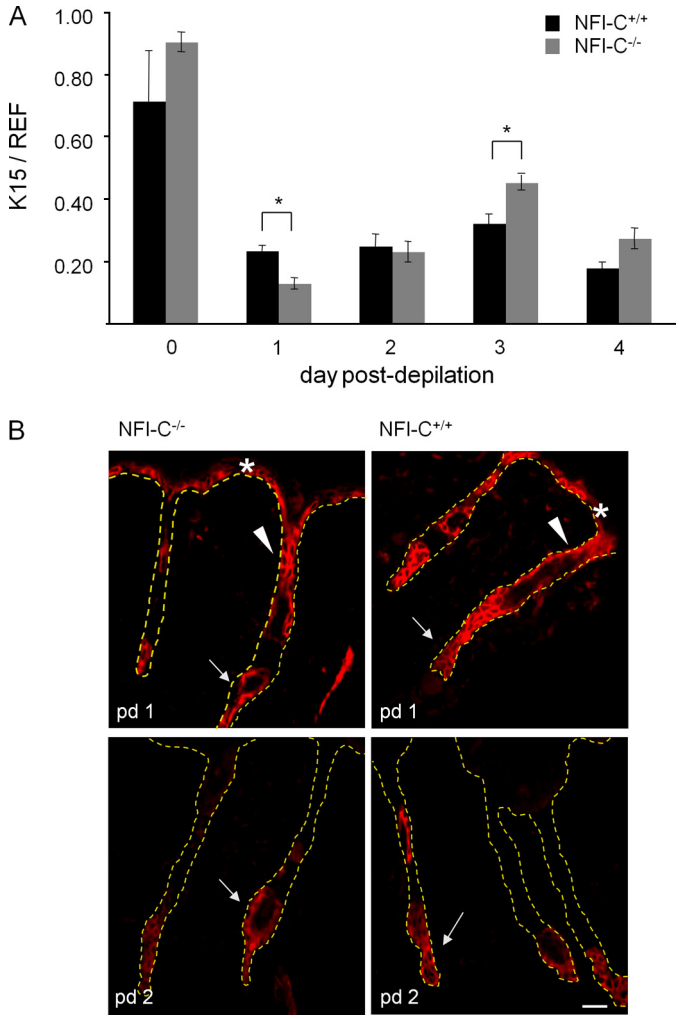

FIGURE 7. **TGF-β1 levels correlate to the amount of K15-positive stem cells.** *A*, expression of K15 relative to reference (*REF*) genes assessed in skin samples by RT-qPCR, decreased at day 1 post-depilation. Different levels of expression were observed in wild-type and knock-out samples at days 1 and 3 (*, $p < 0.05$). *B*, immunofluorescent staining on skin cryosections localized K15 in the basal layer of the epidermis (asterisks), in the ORS (*arrowheads*), and in the region corresponding to the bulge and/or second hair germ (*arrows*) at day 1 post-depilation (*pd 1*). At day 2 post-depilation the staining was limited to the bulge/second hair germ area (*arrows*). No significant difference was seen when comparing cell staining of the two genotypes. *Yellow dashed lines* indicate the limit of keratinocyte layers in the epidermis and hair follicles. *Scale bar*: 30 μm.

affected by the lack of NFI-C, and the increased expressions of PDGF and its receptor α chain were linked to an increased infiltration of macrophages in the skin wounds of knock-out mice. However, a delay of the anagen onset was also observed for the NFI-$C^{-/-}$ animals in the absence of induced hair removal after the first spontaneous telogen phase. This indicates that the hair growth delay is independent of inflammatory or trauma events linked to hair loss during over-grooming or plucking. Moreover, we did not identify a defect of NFI-C-null hair follicle morphogenesis, further strengthening the conclusion that NFI-C regulates one or several events that drive the transition from telogen to anagen.

The expression patterns of various hair cycle makers indicated that the delay occurs before or during early anagen and that it persists throughout the cycle. One of the earliest indications of a progression from telogen toward anagen is a change in BMP4 and Noggin levels. Transition to the proliferation stage has been linked to both BMP down-regulation and Noggin expression increase, releasing bulge stem cells from BMP growth-inhibitory effects (12, 29, 50). BMP4 has been also proposed to keep hair progenitor cells in a quiescent state during telogen by repressing Shh signaling (20). NFI-$C^{-/-}$ mice were found to have unaltered BMP4 and Noggin expression. Rather, the earliest significant molecular defect noted in NFI-$C^{-/-}$ mice was the abnormally low Shh levels and the delay in its rise after plucking. This provides an explanation for the impaired increase of Wnt5a signaling and reduced Lef1 expression that was observed in the anagen stage of knock-out mice. Shh is a mitogenic factor in keratinocytes, and its activation was identified as a key event of the cycle initiation (12).

We also observed a sustained activation of TGF-β1 pathway during telogen phase in NFI-$C^{-/-}$ mice. TGF-β1 and BMP signaling share many structural and functional similarities. They bind to and activate related cell surface receptors with intrinsic kinase activity and thereby stimulate the phosphorylation of Smad proteins (2 and 3 for TGF-β and 1, 5, and 8 for BMP), which in turn form complexes with Smad4 that migrate to the nucleus to activate the transcription of target genes. Our results suggest that Shh gene expression is also regulated by the TGF-β1 pathway in the hair follicle and that high expression of this growth factor in knock-out animals may explain the decrease of Shh expression during early anagen.

The first recognized effect of TGF-β1 overexpression in NFI-$C^{-/-}$ mice is the up-regulation of p21, a cyclin-dependent kinase inhibitor that induces cell cycle arrest. This finding is in agreement with the hair follicle defects found in Smad4 knock-out mice. Smad4 is a common mediator of TGF-β and BMP signaling, and the lack of this protein results in decreased p21 levels and increased cell proliferation in the ORS (51). In contrast with our results, Smad$4^{-/-}$ mice showed a major block in the hair follicle cycle progression that failed to enter the regression phase and persisted in an abnormal anagen phase (52). Therefore, alteration of both TGF-β and BMP pathways leads to a more extensive cell proliferation and compromised cycling, whereas the lack of NFI-C, which affects TGF-β but not BMP4 levels, causes a delayed anagen onset but does not impair cycle progression. The lack of either NFI-C or Smad4 did not affect the development or initiation of the primary hair follicle cycle, indicating that TGF-β/BMP-activated Smad signaling is implicated only in postnatal hair follicle cycling.

A correlation between anagen delay and an increased activity of the TGF-β1 pathway and of p21 expression was recently reported in another mouse model. Lefever *et al.* (53) characterized mice with a keratinocyte-specific deletion of the N-WASP protein, a regulator of cytoplasmic and nuclear actin polymerization that controls epithelial cell motility and gene expression. Whereas NFI-C and N-WASP were not known to control similar biological functions, both knock-out models show a delay in anagen entry. The N-WASP knock-out mice also display more active TGF-β signaling and increased expression of the p21 inhibitor of cell proliferation. Thus, tight regulation of TGF-β pathway by regulatory proteins such as NFI-C and N-WASP may control a critical checkpoint in the telogen-ana-

gen transition. However, N-WASP$^{-/-}$ mice also showed abnormal hair follicle morphogenesis and transient alopecia, and their keratinocytes show an intrinsic growth defect but unaltered Wnt signaling, unlike NFI-C$^{-/-}$ mice. This indicates that different cellular and signaling events contribute to the distinct morphogenesis and follicular cycle phenotypes.

The finding of an interaction between NFI-C and TGF-β signaling is also in agreement with the recent results in skin healing experiments where we have shown that the wound closure was accelerated in NFI-C knock-out animals (9). This phenotype has been linked to the increased recruitment and/or proliferation of fibroblasts as well as their higher differentiation to myofibroblasts whose contraction leads to the closure of the injured area. Differentiation of myofibroblasts was characterized by the onset of the expression of α-smooth muscle actin in response to increased TGF-β signaling, further supporting the role of NFI-C in TGF-β pathway activation.

NFI family proteins were first linked to the control of cell division by the finding that expression of an active Ha-ras mitogen down-regulated NFI-C and other family members (54). Here we find that NFI-C acts consistently to repress p21 expression, an inhibitor of cell division, which may further contribute to the activation of cell proliferation by the mitogen-activated signaling pathway. Ouellet *et al.* (55) found a functional target site for NFI in the promoter of p21 gene, suggesting a direct transcriptional regulation of p21 by the transcription factor. Thus, in addition to its role in decreasing TGF-β expression, whose signaling pathway is known to down-regulate p21 expression, NFI may also act as a direct repressor of p21 expression to trigger keratinocytes to enter the proliferation stage at the onset of anagen. The possibility of an independent regulation of TGF-β1 and p21 by NFI-C is supported by their different expression patterns at day 2 post-depilation, when TGF-β1 levels remain elevated in NFI-C$^{-/-}$ mice, whereas p21 expression is comparable in the two genotypes. This rather suggests a temporally independent repression of the expression of the two proteins by NFI-C. Further studies will be necessary to determine to which extent p21 transcription may be directly controlled by NFI-C or by the indirect repression mediated by the activation of the TGF-β pathway.

The regulatory nexus formed by TGF-β1, p21, and NFI-C is further supported by the occurrence of both tooth and hair-related phenotypes in NFI-C$^{-/-}$ mice. Lack of roots in molar teeth was associated with abnormal differentiation and proliferation of odontogenic cells (8, 56). It has been shown that the loss of NFI-C results in an increase of TGF-β and p-Smad2/3 expression in knock-out aberrant odontoblasts. In addition, NFI-C-deficient primary pulp cells also exhibited an increased expression of p21 and cell growth arrest (8). Thus, in concordance with the defect observed in the follicular stem cells of mutant animals, NFI-C may be more generally involved in controlling the equilibrium between the activation of proliferation *versus* growth arrest and/or differentiation of the stem and progenitor cells that contribute to molar root development and hair follicle regeneration.

Higher expression of TGF-β and p21 readily explains the decreased proliferation of NFI-C$^{-/-}$ keratinocyte progenitor cells at the onset of anagen, as TGF-β is known to inhibit epithelial cell growth and to ellicit a p21-mediated arrest of cells in the G_1 phase of the cell cycle (45, 57). However, it has been recently shown that Smad4$^{-/-}$ mice display a depletion of stem cells during the first hair follicle cycles (52). In contrast, a similar amount of K15-expressing stem cells were found in NFI-C null and control biopsies. Moreover, K15-positive cells are localized in the epidermal basal layer, the ORS, and the secondary hair germ/bulge area during telogen, whereas they are restricted to the secondary germ/bulge region in early anagen, indicating that the distribution of K15 is hair follicle cycle-dependent. This finding may explain the discrepancies in reports localizing K15 exclusively in the stem cell niche or in both the epithelial layer and stem cell niche (46, 47, 58).

Taken together, these findings suggest that NFI-C may have a general role in regulating tissue growth and regeneration processes, as found in the skin, hair follicles, and teeth. Other CTF/NFI family members had been implicated in morphogenesis during development. For instance, NFI-A inhibits the differentiation of hematopoietic stem cells and neurogenic precursors, whereas NFI-B and NFI-X promote the proliferation of hematopoietic cells, and these NFI subtypes have been associated with various developmental abnormalities during embryogenesis (59–62). However, NFI-C appears to play the specific role in the family to control the activation of "adult" progenitor cells and to regulate tissue growth and/or regeneration in post-natal life.

Acknowledgments—We thank Richard M. Gronostajski for providing NFI-C knock-out mice and Ione Gutscher and Armindo Teixeira for excellent technical assistance.

REFERENCES

1. Gronostajski, R. M., Adhya, S., Nagata, K., Guggenheimer, R. A., and Hurwitz, J. (1985) *Mol. Cell. Biol.* **5,** 964–971
2. Roulet, E., Bucher, P., Schneider, R., Wingender, E., Dusserre, Y., Werner, T., and Mermod, N. (2000) *J. Mol. Biol.* **297,** 833–848
3. Gronostajski, R. M. (2000) *Gene* **249,** 31–45
4. das Neves, L., Duchala, C. S., Tolentino-Silva, F., Haxhiu, M. A., Colmenares, C., Macklin, W. B., Campbell, C. E., Butz, K. G., Gronostajski, R. M., and Godinho, F. (1999) *Proc. Natl. Acad. Sci. U.S.A.* **96,** 11946–11951
5. Gründer, A., Ebel, T. T., Mallo, M., Schwarzkopf, G., Shimizu, T., Sippel, A. E., and Schrewe, H. (2002) *Mech. Dev.* **112,** 69–77
6. Driller, K., Pagenstecher, A., Uhl, M., Omran, H., Berlis, A., Gründer, A., and Sippel, A. E. (2007) *Mol. Cell. Biol.* **27,** 3855–3867
7. Steele-Perkins, G., Butz, K. G., Lyons, G. E., Zeichner-David, M., Kim, H. J., Cho, M. I., and Gronostajski, R. M. (2003) *Mol. Cell. Biol.* **23,** 1075–1084
8. Lee, D. S., Park, J. T., Kim, H. M., Ko, J. S., Son, H. H., Gronostajski, R. M., Cho, M. I., Choung, P. H., and Park, J. C. (2009) *J. Biol. Chem.* **284,** 17293–17303
9. Plasari, G., Calabrese, A., Dusserre, Y., Gronostajski, R. M., McNair, A., Michalik, L., and Mermod, N. (2009) *Mol. Cell. Biol.* **29,** 6006–6017
10. Mikkola, M. L. (2007) *Cell Cycle* **6,** 285–290
11. Mikkola, M. L., and Millar, S. E. (2006) *J. Mammary Gland Biol. Neoplasia* **11,** 187–203
12. Botchkarev, V. A., and Kishimoto, J. (2003) *J. Investig. Dermatol. Symp. Proc.* **8,** 46–55
13. Cotsarelis, G., Kaur, P., Dhouailly, D., Hengge, U., and Bickenbach, J. (1999) *Exp. Dermatol.* **8,** 80–88
14. Müller-Röver, S., Handjiski, B., van der Veen, C., Eichmüller, S., Foitzik, K., McKay, I. A., Stenn, K. S., and Paus, R. (2001) *J. Invest. Dermatol.* **117,** 3–15
15. Paus, R., and Cotsarelis, G. (1999) *N. Engl. J. Med.* **341,** 491–497
16. Budd, P. S., Antoniou, J., Mellor, A. L., and Jackson, I. J. (1997) *Mamm.*

Genome **8,** 631–635
17. Nordlund, J. J. (2007) *Dermatol. Clin.* **25,** 271–281
18. Cotsarelis, G., Sun, T. T., and Lavker, R. M. (1990) *Cell* **61,** 1329–1337
19. Lavker, R. M., Sun, T. T., Oshima, H., Barrandon, Y., Akiyama, M., Ferraris, C., Chevalier, G., Favier, B., Jahoda, C. A., Dhouailly, D., Panteleyev, A. A., and Christiano, A. M. (2003) *J. Investig. Dermatol. Symp. Proc.* **8,** 28–38
20. Botchkarev, V. A., Botchkareva, N. V., Nakamura, M., Huber, O., Funa, K., Lauster, R., Paus, R., and Gilchrest, B. A. (2001) *FASEB J.* **15,** 2205–2214
21. Huelsken, J., Vogel, R., Erdmann, B., Cotsarelis, G., and Birchmeier, W. (2001) *Cell* **105,** 533–545
22. Reddy, S., Andl, T., Bagasra, A., Lu, M. M., Epstein, D. J., Morrisey, E. E., and Millar, S. E. (2001) *Mech. Dev.* **107,** 69–82
23. Sano, S., Kira, M., Takagi, S., Yoshikawa, K., Takeda, J., and Itami, S. (2000) *Proc. Natl. Acad. Sci. U.S.A.* **97,** 13824–13829
24. Sato, N., Leopold, P. L., and Crystal, R. G. (1999) *J. Clin. Invest.* **104,** 855–864
25. Blanpain, C., Lowry, W. E., Geoghegan, A., Polak, L., and Fuchs, E. (2004) *Cell* **118,** 635–648
26. Alonso, L., and Fuchs, E. (2003) *Proc. Natl. Acad. Sci. U.S.A.* **100,** 11830–11835
27. Andl, T., Ahn, K., Kairo, A., Chu, E. Y., Wine-Lee, L., Reddy, S. T., Croft, N. J., Cebra-Thomas, J. A., Metzger, D., Chambon, P., Lyons, K. M., Mishina, Y., Seykora, J. T., Crenshaw, E. B., 3rd, and Millar, S. E. (2004) *Development* **131,** 2257–2268
28. Botchkarev, V. A., Botchkareva, N. V., Sharov, A. A., Funa, K., Huber, O., and Gilchrest, B. A. (2002) *J. Invest. Dermatol.* **118,** 3–10
29. Zhang, J., He, X. C., Tong, W. G., Johnson, T., Wiedemann, L. M., Mishina, Y., Feng, J. Q., and Li, L. (2006) *Stem Cells* **24,** 2826–2839
30. Foitzik, K., Lindner, G., Mueller-Roever, S., Maurer, M., Botchkareva, N., Botchkarev, V., Handjiski, B., Metz, M., Hibino, T., Soma, T., Dotto, G. P., and Paus, R. (2000) *FASEB J.* **14,** 752–760
31. Jacobs, W. L. (1971) *Clin. Chim. Acta* **31,** 175–179
32. Persijn, J. P., van der Slik, W., and Zwart, W. A. (1971) *Clin. Chim. Acta* **35,** 239–240
33. Karlen, Y., McNair, A., Perseguers, S., Mazza, C., and Mermod, N. (2007) *BMC Bioinformatics* **8,** 131
34. Argyris, T. S. (1968) *Adv. Morphog.* **7,** 1–43
35. Müller-Röver, S., Tokura, Y., Welker, P., Furukawa, F., Wakita, H., Takigawa, M., and Paus, R. (1999) *Exp. Dermatol.* **8,** 237–246
36. Cameron, R., Kellen, J., Kolin, A., Malkin, A., and Farber, E. (1978) *Cancer Res.* **38,** 823–829
37. De Young, L. M., Richards, W. L., Bonzelet, W., Tsai, L. L., and Boutwell, R. K. (1978) *Cancer Res.* **38,** 3697–3701
38. Kawabe, T. T., Kubicek, M. F., Johnson, G. A., and Buhl, A. E. (1994) *J. Invest. Dermatol.* **103,** 122–126
39. Handjiski, B. K., Eichmüller, S., Hofmann, U., Czarnetzki, B. M., and Paus, R. (1994) *Br. J. Dermatol.* **131,** 303–310
40. Chiang, C., Swan, R. Z., Grachtchouk, M., Bolinger, M., Litingtung, Y., Robertson, E. K., Cooper, M. K., Gaffield, W., Westphal, H., Beachy, P. A., and Dlugosz, A. A. (1999) *Dev. Biol.* **205,** 1–9
41. St-Jacques, B., Dassule, H. R., Karavanova, I., Botchkarev, V. A., Li, J., Danielian, P. S., McMahon, J. A., Lewis, P. M., Paus, R., and McMahon, A. P. (1998) *Curr. Biol.* **8,** 1058–1068
42. DasGupta, R., and Fuchs, E. (1999) *Development* **126,** 4557–4568
43. Liu, X., Driskell, R. R., Luo, M., Abbott, D., Filali, M., Cheng, N., Sigmund, C. D., and Engelhardt, J. F. (2004) *J. Invest. Dermatol.* **123,** 264–274
44. Filali, M., Cheng, N., Abbott, D., Leontiev, V., and Engelhardt, J. F. (2002) *J. Biol. Chem.* **277,** 33398–33410
45. Yue, J., and Mulder, K. M. (2001) *Pharmacol. Ther.* **91,** 1–34
46. Cotsarelis, G. (2006) *J. Invest. Dermatol.* **126,** 1459–1468
47. Werner, S., and Munz, B. (2000) *Exp. Cell Res.* **254,** 80–90
48. Matsuo, K., Mori, O., and Hashimoto, T. (2003) *Arch. Dermatol. Res.* **295,** 33–37
49. Tomita, Y., Akiyama, M., and Shimizu, H. (2006) *J. Dermatol. Sci.* **43,** 105–115
50. Kobielak, K., Pasolli, H. A., Alonso, L., Polak, L., and Fuchs, E. (2003) *J. Cell Biol.* **163,** 609–623
51. Qiao, W., Li, A. G., Owens, P., Xu, X., Wang, X. J., and Deng, C. X. (2006) *Oncogene* **25,** 207–217
52. Yang, L., Mao, C., Teng, Y., Li, W., Zhang, J., Cheng, X., Li, X., Han, X., Xia, Z., Deng, H., and Yang, X. (2005) *Cancer Res.* **65,** 8671–8678
53. Lefever, T., Pedersen, E., Basse, A., Paus, R., Quondamatteo, F., Stanley, A. C., Langbein, L., Wu, X., Wehland, J., Lommel, S., and Brakebusch, C. (2010) *J. Cell Sci.* **123,** 128–140
54. Nebl, G., Mermod, N., and Cato, A. C. (1994) *J. Biol. Chem.* **269,** 7371–7378
55. Ouellet, S., Vigneault, F., Lessard, M., Leclerc, S., Drouin, R., and Guérin, S. L. (2006) *Nucleic Acids Res.* **34,** 6472–6487
56. Park, J. C., Herr, Y., Kim, H. J., Gronostajski, R. M., and Cho, M. I. (2007) *J. Periodontol.* **78,** 1795–1802
57. Viallard, J. F., Lacombe, F., Belloc, F., Pellegrin, J. L., and Reiffers, J. (2001) *Cancer Radiother.* **5,** 109–129
58. Liu, Y., Lyle, S., Yang, Z., and Cotsarelis, G. (2003) *J. Invest. Dermatol.* **121,** 963–968
59. Campbell, C. E., Piper, M., Plachez, C., Yeh, Y. T., Baizer, J. S., Osinski, J. M., Litwack, E. D., Richards, L. J., and Gronostajski, R. M. (2008) *BMC Dev. Biol.* **8,** 52
60. Chaudhry, A. Z., Lyons, G. E., and Gronostajski, R. M. (1997) *Dev. Dyn.* **208,** 313–325
61. Kralovics, R., Guan, Y., and Prchal, J. T. (2002) *Exp. Hematol.* **30,** 229–236
62. Rosa, A., Ballarino, M., Sorrentino, A., Sthandier, O., De Angelis, F. G., Marchioni, M., Masella, B., Guarini, A., Fatica, A., Peschle, C., and Bozzoni, I. (2007) *Proc. Natl. Acad. Sci. U.S.A.* **104,** 19849–19854